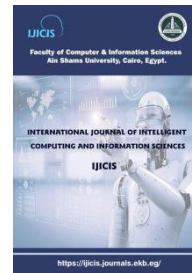




International Journal of Intelligent Computing and Information Sciences

<https://ijicis.journals.ekb.eg/>



An Optimal Similarity Neutrosophic Model Based on Distance Measuring to Improving Content-based Image Retrieval

A.E. Amin*

Department of Computer Science, Mansoura University, Mansoura 35516, Egypt

ahmedel_sayed@mans.edu.eg

Received 2021- 06-29; Revised 2021-09-30; Accepted 2021-10-12

Abstract:

This paper deals with images using the theory of neutrosophic, which the idea of working, on set about the degree of truth, indeterminacy, and falsity. Which helped to discover the hidden features of the images that were segmented by using neutrosophic image processing into objects and then extracting the features into the three truth, indeterminacy, and falsity levels of the image and combining these features to extract the original image features.

The proposed similarity model namely weighted Hamming distance measure that based on the single-value neutrosophic set was used to retrieve images from the database, by matching with the query image that extracted its feature in the same way.

The results showed that the proposed system is highly efficient in retrieving images compared to different distance measures such as Euclidian, Manhattan, and Minkowski.

Finally, A novel similarity model used to match the neutrosophic image features for CBIRs. In the proposed system, an image is segmented into objects, edges, and backgrounds by using neutrosophic image processing.

Key words: *Neutrosophic image processing; Single-valued neutrosophic similarity; Neutrosophic theory*

1. Introduction:

Content based image retrieval systems (CBIRs) [1] are among the systems that have helped in areas such as engineering, education, trade, etc. [2]. The results have shown impressive in these areas over the past several years [3]. These systems rely on the way they work to save the features extracted from the images in a database to be retrieved by matching the features of the query image with the features stored in the database through different similarities methods [4]. There are many ways to extract features from images [5], for example, but not limited to the colors, textures and regions. And through the application emerged the advantages and disadvantages of each method [6]. One of the

* Corresponding author: A.E. Amin

Department of Computer Science, Mansoura University, Mansoura 35516, Egypt

E-mail address: ahmedel_sayed@mans.edu.eg

most important disadvantages that have been worked on in this area is the overlap of the objects that constructed the images. The similarities methods used in the retrieval image from image database includes Minkowski and standard measures [7], statistical measures [8], divergence measures [9], and other measures [10]. One of the most important problems faced by these methods is the uncertainty areas and ways of identifying them in the databases.

Neuroscientific studies [11] have recently emerged, which is a new philosophy that extends fuzzy logic and is the basis of neutrosophic logic, probability and statistics, which study the origin, nature and scope of nature and their interactions with different spectra [12].

Through the definition of neutrosophic, which is defined as a set about the degree of truth, indeterminacy, and falsity [13]. Single-valued neutrosophic sets (SVNS) [14] were used for ease of expression in the proposed image retrieval system to resolve the problem of overlapping objects in the image as well as to identify uncertainly regions in images.

The remainder of this research is organized as follows: The second section presents a theoretical background on the neutrosophic axioms. In third section, the proposed system summarization. Use of neutrosophic theory in image processing to segmented the image according to its objects in the fourth section. Then extract the features from the segmented images that produced from the original images and clustered them to derive the original image features in section five. In the sixth section, an optimal neutrosophic similarity model was applied to retrieve the images. Section seven presents the experimental work, while the results and discussion were discussed in section eight with comparison of the proposed model for similarity in the proposed system with the other distance measures.

2. Neutrosophic axioms:

For a discourse universe (X) with a generic element in X denoted by x . Both of membership of truth $T_A(x)$, indeterminacy $I_A(x)$, and falsity $F_A(x)$ for $(A \text{ NS } A)$ on X is defined by [15]:

$$\begin{aligned} T_A(x): X &\rightarrow]0^-, 1^+[\\ I_A(x): X &\rightarrow]0^-, 1^+[\\ F_A(x): X &\rightarrow]0^-, 1^+[\end{aligned}$$

$$\text{where; } 0^- \leq \sup T_A(x) + \sup I_A(x) + \sup F_A(x) \leq 3^+$$

Whereas the membership of both truth, indeterminacy, and falsity of single-valued neutrosophic set (SVNS) are defined by [14]:

$$\begin{aligned} T_A(x): X &\rightarrow [0, 1] \\ I_A(x): X &\rightarrow [0, 1] \\ F_A(x): X &\rightarrow [0, 1] \end{aligned}$$

$$\text{where; } 0 \leq \sup T_A(x) + \sup I_A(x) + \sup F_A(x) \leq 3$$

Assume that, A and B are SVNS, represented as:

$$A = \langle T_A, I_A, F_A \rangle, \quad B = \langle T_B, I_B, F_B \rangle$$

Then, the normalize Humming distance measure (D^H) between A and B is [16]:

$$D^H(A, B) = \frac{1}{3} (|T_A - T_B| + |I_A - I_B| + |F_A - F_B|)$$

3. Proposed method:

The proposed method for image retrieval passes through three main phases as shown in figure 1. First, generate the database for images, the features for all images that extracted by the neutrosophic theory are stored in the database.

Where the images are segmented to objects, for each object features are extracted in three levels are truth, indeterminacy, and falsity. All levels features are clustered to get the original image features. Secondly, neutrosophic features are extracted to query image as the same way of all images features are extracted. Finally, the weighted humming distance measure used to retrieve the query image from the database of images.

4. Neutrosophy Image Processing:

Depending on the idea of neutrosophic, images are treated, where the image is divided into three main elements are objects, background and blurry edges. All elements can be defined as T, F and I respectively. Where T is the degree of membership, F is the degree of non-membership and I is the degree of indeterminacy. Neutrosophy image (NS^{Im}) processing is achieved by seven phases are:

4.1. Image pre-processing:

The inherent complexity of gray level images such as brightness, contrast, edges, shape, contours, texture, perspective, shadows, and so on, is lower than that of color images. So, color images are converted to grayscale image where gray images contain one domain. The gray image pixel's is represented by an integer between 0 and 255, i.e., using function \mathcal{F} to convert color image $\mathbb{R}^{n \times m \times 3}$ to grayscale image $\mathbb{R}^{n \times m}$.

4.1.1. Neutrosophic Image Domain:

The digital image Domain (D^{Im}) is converted to (NS^{Im}) where a pixel $P(i, j)$ in the image is described as $P(T, I, F)$. The meaning of $P(T, I, F)$ that each pixel belongs to its intensity by its t% is true, i% is indeterminate and f% is false. That achieved by the following steps [17]:

4.1.2. Determine membership and non-membership degree (T and F):

The position of each pixel in an image is determined as $(P(x, y))$. Depending on the size of the image, the size of the main filter ($N \times N$), that used to remove the noise and make image uniform is determined. Then, the S-function is used to map the intensity domain of the image (D_{xy}^{Im}) to new domain (ND_{xy}^{Im}) as [18]:

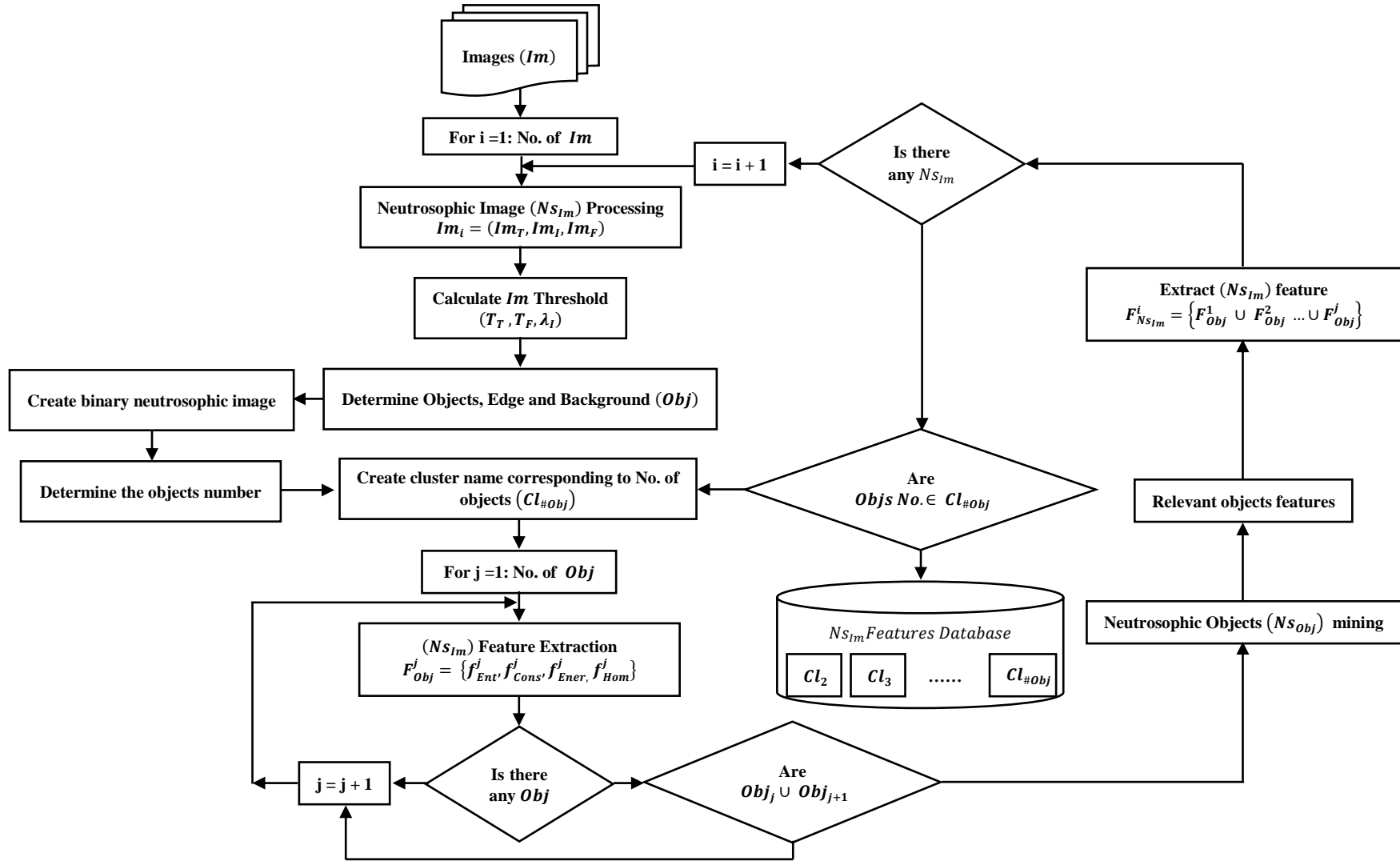


Fig.1: The proposed method for image retrieval system.

$$ND_{xy}^{Im} = S(D_{xy}^{Im}, a, b, c) = \begin{cases} 0 & 0 \leq D_{xy}^{Im} \leq a \\ \frac{(D_{xy}^{Im} - a)^2}{(b - a)(c - a)} & a \leq D_{xy}^{Im} \leq b \\ 1 - \frac{(D_{xy}^{Im} - c)^2}{(c - b)(c - a)} & b \leq D_{xy}^{Im} \leq c \\ 1 & D_{xy}^{Im} \geq c \end{cases}$$

The parameters a, b and c values are calculated by algorithm based on histogram [19] as:

1. Calculate image histogram (Im_{Hist}).
2. Dividing (Im_{Hist}) to regions according the local maxima; $\{Im_{Hist}(R_1), Im_{Hist}(R_2), \dots, Im_{Hist}(R_n)\}$. Then, calculate the mean of local maxima regions as:

$$\overline{Im_{Hist}(R)} = \frac{\sum_{i=1}^n Im_{Hist}(R_i)}{n}$$

3. Let first peak region be (R_{min}^P) and the last be (R_{max}^P); then find the peak greater than ($\overline{Im_{Hist}(R)}$).
4. Define low limit boundary (B_L) and upper limit boundary (B_U) as:

$$\sum_{i=R_{min}^P}^{B_L} Im_{Hist}(i) = f_1$$

$$\sum_{i=B_U}^{R_{max}^P} Im_{Hist}(i) = f_1$$

Where the lost information was allowed in the range $[R_{min}^P, B_L]$ and $[B_U, R_{max}^P]$, and f_1 is constant (in experimental $f_1 = 0.0001$).

5. Determine the parameter a and c by:

$$a = (1 - f_2)(R_1^P - R_{min}^P) + R_{min}^P$$

$$\text{if } (a > B_L) \text{ Then } a = B_L$$

$$c = f_2(R_{max}^P - R_n^P) + R_n^P$$

$$\text{if } (c > B_U) \text{ Then } c = B_U$$

6. The maximum entropy (En_{max}) principle [20] is used to calculate the parameter b, where the optimal b will generate the largest $En_{max}(x)$ from:

$$En_{max}(X, a, b_{opt}, c) = \text{Max}\{En[X; a, b, c] | R_{min}^P \leq a < b < c \leq R_{max}^P\}$$

Where the more information contained in the image, is the greater the entropy as shown in formula:

$$En(x) = \frac{1}{M \times N} \sum_{i=1}^M \sum_{j=1}^N Sh_n(ND_{xy}^{Im}(x, y))$$

Where; Sh_n is a Shannon function [21] defined as:

$$Sh_n(T(x, y)) = -T(x, y) \log_2 T(x, y) - [1 - T(x, y)] \log_2 (1 - T(x, y))$$

Where $x = 1, 2, \dots, M$ and $y = 1, 2, \dots, N$

4.1.3. Neutrosophic image enhancement:

When the new intensity domain of the image is determined, the new range is enhanced using the intensification transformation [22] as:

$$NS_T^{lm} = E(T(x, y)) = \begin{cases} 2T^2(x, y) & 0 \leq T(x, y) \leq 0.5 \\ 1 - 2(1 - T(x, y))^2 & 0.5 \leq T(x, y) \leq 1 \end{cases}$$

$$NS_F^{lm} = F_E(x, y) = 1 - T_E(x, y)$$

4.1.3.1. Thresholding calculation:

The purpose of the image enhancement process is to provide better visual appearance and improve quality, using a combination of techniques such as: algorithms based on the human visual system [23], histograms with hue-preservation [24], JPEG-based enhancement for the visually impaired [25], and histogram modification techniques [26]. A heuristic approach is used to improve the image by identifying the thresholds that separate the new domains NS_T^{lm} and NS_F^{lm} as shown in the figure 2.

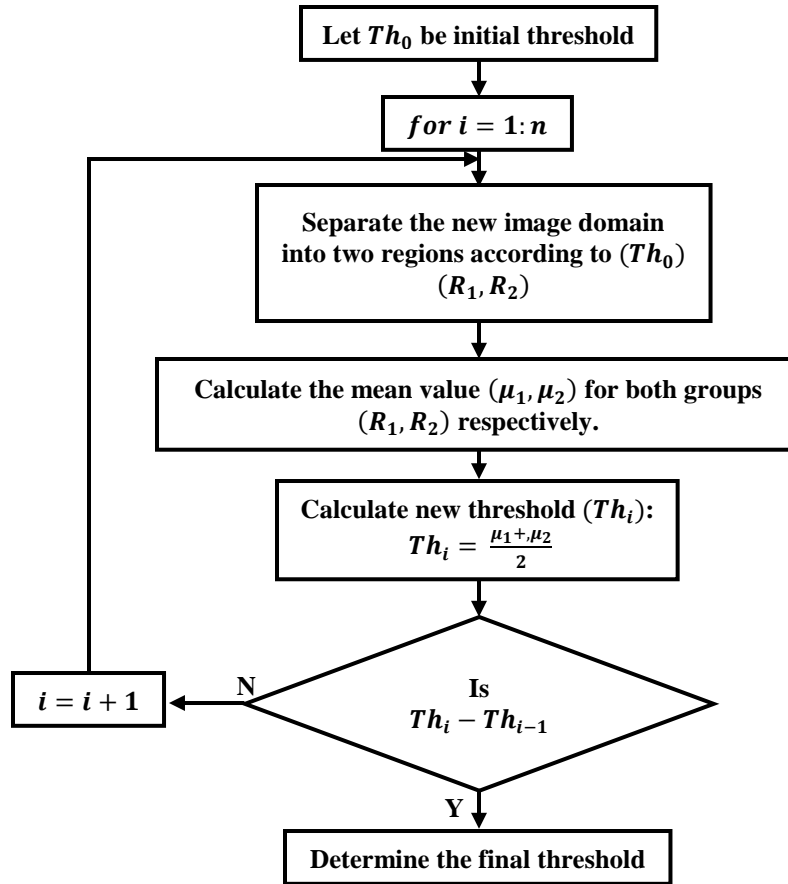


Figure 2: flowchart to determine the image domain threshold.

4.1.3.2. Determine indeterminacy (I):

When segmenting images, the texture features of the image play an important role. These are the differences in the intensity of the pixels that embedded in the objects, the background and the uncertainty areas by the image. The variation of pixel intensity can be represented by homogeneity while the change in gray levels represents by the uncertainty areas [27].

The procedure that achieved to determine the indeterminacy (I) as shown in figure 3 is:

- Calculate the standard deviation of pixel $P(i, j)$ by using a $k \times k$ window have a center (x, y) as the formula:

$$SD(x, y) = \left[\frac{\sum_{p=x-(k-1)/2}^{x+(k+1)/2} \sum_{q=y-(k-1)/2}^{y+(k+1)/2} (g_{pq} - \mu_{xy})^2}{k^2} \right]^{0.5}$$

Where the mean of the intensity value (μ_{xy}) within the window is:

$$\mu_{xy} = \frac{\sum_{p=x-\frac{k-1}{2}}^{x+\frac{k+1}{2}} \sum_{q=y-\frac{k-1}{2}}^{y+\frac{k+1}{2}} g_{pq}}{k^2}$$

where g_{pq} is location pixel intensity

- Sobel operator [28] is used to calculate the uncertainty of pixels ($P(i, j)$) as:

$$U(x, y) = \sqrt{G_x^2 + G_y^2}$$

Where the horizontal and vertical derivative approximation are G_x and G_y respectively.

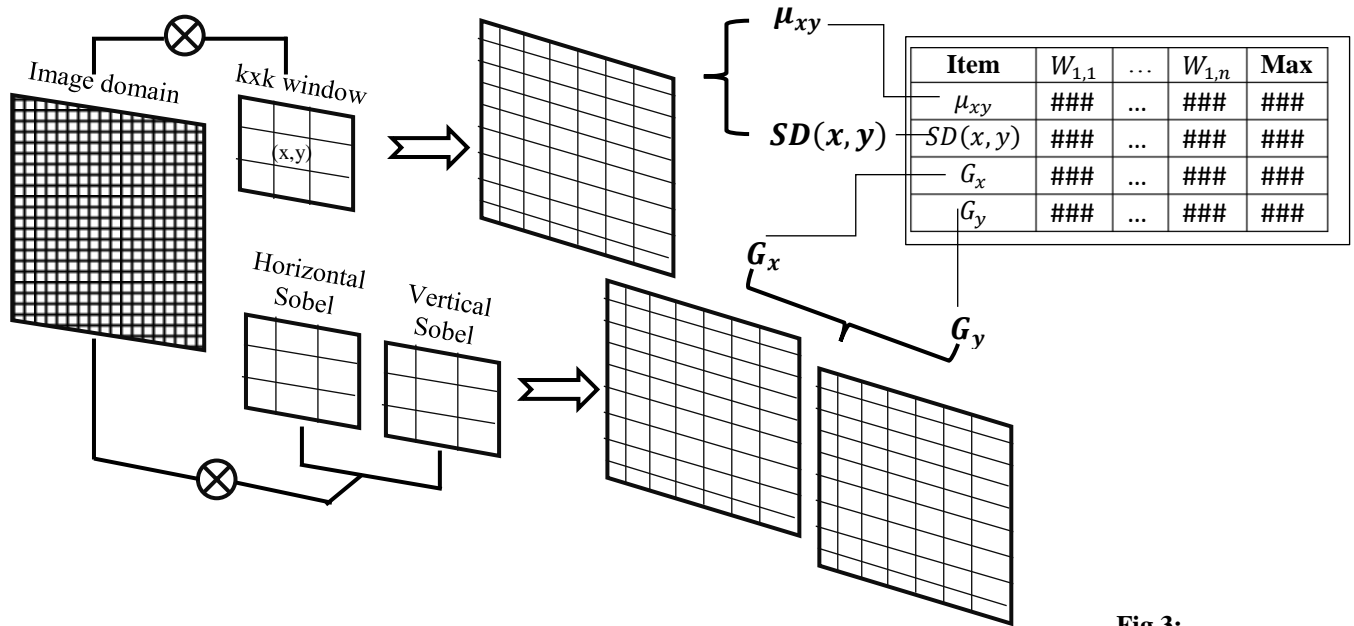


Fig.3:

indeterminacy procedure.

- The homogeneity is defined as normalization both of standard deviation and uncertainty as:

$$H(x, y) = 1 - [(SD(x, y)/SD_{max}) \times (U(x, y)/U_{max})]$$

Where $SD_{max} = \text{Max}\{SD(x, y)\}$ and $U_{max} = \text{Max}\{U(x, y)\}$

- Indeterminacy (I) can represents as:

$$NS_I^{Im}(x, y) = 1 - H(x, y)$$

Then the digital image can be represented as a neutrosophic image:

$$NS^{Im} = \{NS_T^{Im}, NS_I^{Im}, NS_F^{Im}\}$$

4.1.3.3. Neutrosophic image segmentation:

The image can be divided according to membership degree, non-membership degree and indeterminacy as an objects, edges, and background respectively. They are defined as [29]:

$$\begin{aligned}
Object (O) &= \begin{cases} true & NS_T^{Im}(x,y) \geq Th_T, NS_I^{Im} < Th_I \\ false & Others \end{cases} \\
Edge (E) &= \begin{cases} true & NS_T^{Im}(x,y) < Th_T \cup NS_F^{Im} < Th_f, NS_I^{Im} \geq Th_I \\ false & Others \end{cases} \\
Background (B) &= \begin{cases} true & NS_F^{Im}(x,y) \geq Th_F, NS_I^{Im} < Th_I \\ false & Others \end{cases}
\end{aligned}$$

Where Th_T and Th_F are the thresholds computed as shown in figure 2, and Th_I is constant (=0.0001).

4.2. Neutrosophic binary image:

For further processing, the images are converted to the binary (BNS^{Im}), so both of the objects (O) and background (B) are mapped to 0 and the edges (E) are mapped to 1 as follows [30]:

$$BNS^{Im} = \begin{cases} 0 & O(x,y) \cup B(x,y) \cup \overline{E(x,y)} = true \\ 1 & Others \end{cases}$$

4.2.1. Determine optimal segmentation boundaries:

For finding optimal segmentation boundaries in the obtained binary image, there are several algorithms are used [31]. One of the good algorithms is the watershed algorithm [32] that shown in figure 4. The following example illustrates an application of the watershed algorithm, assuming there is an overlap between two objects in a binary image (e.g. two circles) as shown in figure 5:

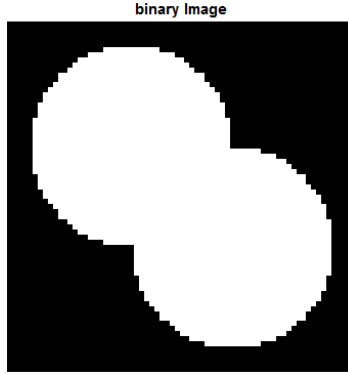


Fig. 5: Overlapping between two objects (circles)

The watershed algorithm is applied to computes a label matrix identifying the watershed regions. The elements of label matrix values greater than or equal to zero don't belong to a unique watershed region that called watershed pixels. Whereas the elements labeled one belong to first region, the elements labeled two belong to the second watershed region.

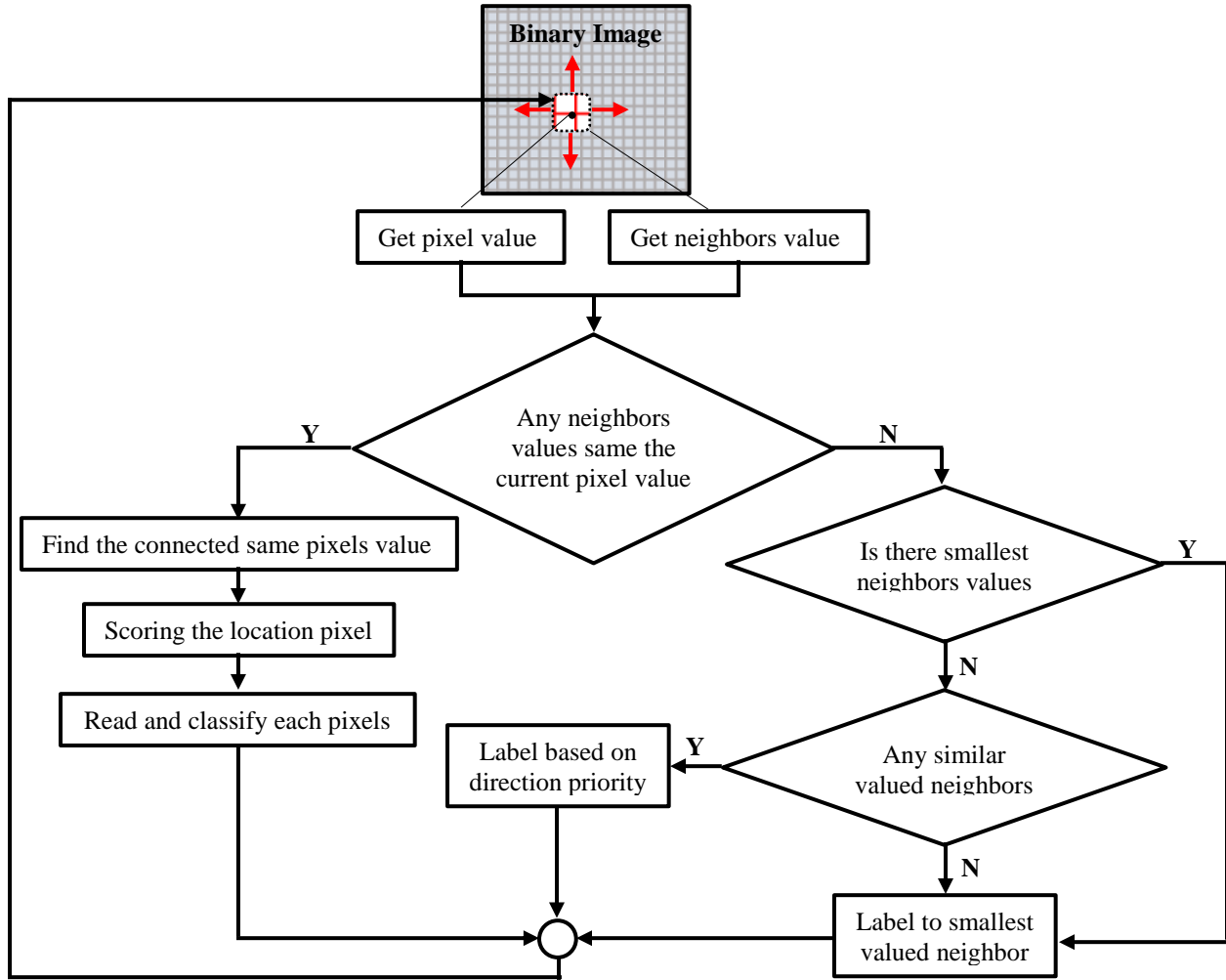


Fig. 4: watershed algorithm flowchart.

After watershed transform completed the resulting label matrix as an RGB image as shown in figure 6.

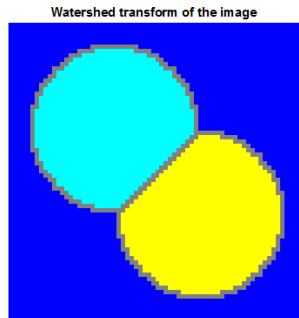


Fig. 6: image segmented by watershed algorithm.

5. Feature Extraction:

The Gray Level Co-occurrence Matrix (*GLCM*) [33] that belongs to texture features methods is used to extract the feature from the (NS^{Im}). The *GLCM* method is used to

determine intensity values and distribution of this intensity. Feature vector that extracted by GLCM can represented as [34]:

$$NS_{Feat.}^{Im} = \{NS_{Ent}^{Im}, NS_{Cont}^{Im}, NS_{Enr}^{Im}, NS_{Homo}^{Im}\}$$

5.1. Neutrosophic image entropy (NS_{Ent}^{Im}):

Entropy is characterized by taking into account the probability of the event contained information and not just the meaning of the event. The neutrosophic set entropy will defined as:

$$\begin{aligned} NS_{Ent}^{Im} &= (NS_{ENT_T}^{Im} + NS_{ENT_I}^{Im} + NS_{ENT_F}^{Im}) \\ \text{Where;} \quad NS_{ENT_T}^{Im} &= \sum_i \sum_j P_T(i, j) \log P_T(i, j) \\ NS_{ENT_I}^{Im} &= \sum_i \sum_j P_I(i, j) \log P_I(i, j) \\ NS_{ENT_F}^{Im} &= \sum_i \sum_j P_F(i, j) \log P_F(i, j) \end{aligned}$$

5.2. Neutrosophic image contrast (NS_{Cont}^{Im}):

The Contrast describe the difference between intensity contrast between a pixel and its neighbor over the whole image. The neutrosophic set contrast can be defined as:

$$\begin{aligned} NS_{Cont}^{Im} &= (NS_{Cont_T}^{Im} + NS_{Cont_I}^{Im} + NS_{Cont_F}^{Im}) \\ \text{Where;} \quad NS_{Cont_T}^{Im} &= \sum_i \sum_j (i - j)^2 P_T(i, j) \\ NS_{Cont_I}^{Im} &= \sum_i \sum_j (i - j)^2 P_I(i, j) \\ NS_{Cont_F}^{Im} &= \sum_i \sum_j (i - j)^2 P_F(i, j) \end{aligned}$$

5.3. Neutrosophic image energy (NS_{Enr}^{Im}):

Energy is used to describe a measure of "information" when formulating an operation under a probability framework. In the neutrosophic image domain can be defined as:

$$\begin{aligned} NS_{Enr}^{Im} &= NS_{Enr_T}^{Im} + NS_{Enr_I}^{Im} + NS_{Enr_F}^{Im} \\ \text{Where;} \quad NS_{Enr_T}^{Im} &= \sum_i \sum_j P_T^2(i, j) \\ NS_{Enr_I}^{Im} &= \sum_i \sum_j P_I^2(i, j) \\ NS_{Enr_F}^{Im} &= \sum_i \sum_j P_F^2(i, j) \end{aligned}$$

5.4. Neutrosophic image homogeneity (NS_{Homo}^{Im}):

The image's homogeneity can be defined as the texture of the image (i.e. the information contained in the image by the intensity of the pixel) except for the edges or corners that changes the intensity from pixel to its neighbor. So the neutrosophic homogeneity measure is the value that measures the closeness of pixels intensity distribution as follows:

$$\begin{aligned} NS_{Homo}^{Im} &= NS_{Homo_T}^{Im} + NS_{Homo_I}^{Im} + NS_{Homo_F}^{Im} \\ \text{Where;} \quad NS_{Homo_T}^{Im} &= \sum_i \sum_j \frac{P_T(i, j)}{1 + |i - j|} \\ NS_{Homo_I}^{Im} &= \sum_i \sum_j \frac{P_I(i, j)}{1 + |i - j|} \end{aligned}$$

$$NS_{Homo_F}^{Im} = \sum_i \sum_j \frac{P_F(i, j)}{1 + |i - j|}$$

From the above, the image is segmented into a group of objects for each object whose features are calculated, and the image features are a vector composed of a union of objects features of the image as shown in figure 7:

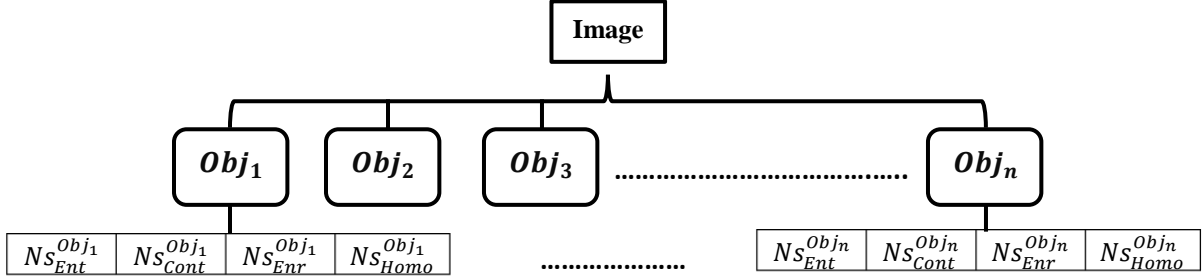


Fig. 7: feature extracted from image objects.

$$NS_{Feat.}^{Im} = \{NS_{Feat.}^{Obj1} \cup NS_{Feat.}^{Obj2} \cup \dots \cup NS_{Feat.}^{Objn}\}$$

$$NS_{Feat.}^{Im} = \{NS_{Ent}^{Obj1}, NS_{Cont}^{Obj1}, NS_{Enr}^{Obj1}, NS_{Homo}^{Obj1}, \dots, NS_{Ent}^{Objn}, NS_{Cont}^{Objn}, NS_{Enr}^{Objn}, NS_{Homo}^{Objn}\}$$

6. Similarity Neutrosophic Model:

The similarity is the measure of how much alike between two vectors of features, one is the query feature and the other, a database of images features. The smaller the similarity measure value, the greater the degree of similarity and vice versa. There are many similarity measures, one of them is distance measures [35]. The distance similarity measures are varies depending on features types such Euclidean Distance, Minkowski Distance, Manhattan Distance, and humming distance [36]. The humming distance is a similarity measure is in the range of [0 1], that is used in the proposed system to its suitability the extracted attributes of binary images.

6.1. The Weighted Hamming Distance Measure Method:

Let the size of images features database $NS_{Feat.}^{Im} = NS_{Feat_{ij}}^{Obj_k}$ be $m \times n$ where the number of objects in the image is Obj_k and from its features the single-valued neutrosophic features matrix (SVNsFM) is built. The value of each element in SVNsFM consists of $\langle NS_{T_{ij}}^{Im}, NS_{I_{ij}}^{Im}, NS_{F_{ij}}^{Im} \rangle$ that expressed by SVNns. Suppose that there is a feature of query:

$$(NS_{Feat.}^Q)_{mn} = \{NS_{Ent}^{Q-Obj1}, NS_{Cont}^{Q-Obj1}, NS_{Enr}^{Q-Obj1}, NS_{Homo}^{Q-Obj1}, \dots, NS_{Ent}^{Q-Objn}, NS_{Cont}^{Q-Objn}, NS_{Enr}^{Q-Objn}, NS_{Homo}^{Q-Objn}\}$$

The similarity between $NS_{Feat.}^{Im}$ and $NS_{Feat.}^Q$ is defined by:

$$d(NS_{Feat.}^{Im}, NS_{Feat.}^Q) = \sum_{k=1}^S \lambda_k \sum_{i=1}^m \sum_{j=1}^n w_j d(NS_{Feat_{ij}}^{Im}, NS_{Feat_{ij}}^Q) \quad \dots (1)$$

Where; λ_k is the weight of each image in the database ($= \frac{1}{S}$, S is No. of images in database), and

$$d(NS_{Feat_{ij}}^{Im}, NS_{Feat_{ij}}^Q) = \frac{1}{3} (|NS_{T_{ij}}^{Im} - NS_{T_{ij}}^Q| + |NS_{I_{ij}}^{Im} - NS_{I_{ij}}^Q| + |NS_{F_{ij}}^{Im} - NS_{F_{ij}}^Q|) \quad \dots (2)$$

To evaluate the best alternative, the ideal point (α^{IP}) that known weight although does not exist in the real world, it does provide an effective way, is used to calculate the optimal weight. So, the SVN ideal point is $\alpha^{IP} = \{t^{IP}, i^{IP}, f^{IP}\} = \{1, 0, 0\}$. Based on the ideal SVN, the single valued neutrosophic positive ideal solution (SVNPIS). A SVNPIS for n objects features is defined by:

$$\alpha^{IP} = \{\alpha_1^{IP}, \alpha_2^{IP}, \dots, \alpha_n^{IP}\}$$

For the feature of image database that consists of (S) images with (n) features be:

Table 1: images features extracted model

Image	<i>Obj₁</i>				<i>Obj_n</i>			
	$NS_{Ent}^{Im^1}$	$NS_{Cont}^{Im^1}$	$NS_{Enr}^{Im^1}$	$NS_{Homo}^{Im^1}$		$NS_{Ent}^{Im^S}$	$NS_{Cont}^{Im^S}$	$NS_{Enr}^{Im^S}$	$NS_{Homo}^{Im^S}$
1	$\langle 0.5, 0.3, 0.1 \rangle$	$\langle 0.6, 0.2, 0.4 \rangle$	$\langle 0.5, 0.3, 0.1 \rangle$	$\langle 0.5, 0.3, 0.1 \rangle$...	$\langle 0.5, 0.3, 0.1 \rangle$	$\langle 0.5, 0.3, 0.1 \rangle$	$\langle 0.5, 0.3, 0.1 \rangle$	$\langle 0.5, 0.3, 0.1 \rangle$
2	$\langle 0.5, 0.3, 0.1 \rangle$	$\langle 0.8, 0.4, 0.6 \rangle$	$\langle 0.5, 0.3, 0.1 \rangle$	$\langle 0.5, 0.3, 0.1 \rangle$...	$\langle 0.5, 0.3, 0.1 \rangle$	$\langle 0.5, 0.3, 0.1 \rangle$	$\langle 0.5, 0.3, 0.1 \rangle$	$\langle 0.5, 0.3, 0.1 \rangle$
.	\vdots
.	\vdots
.	\vdots
n	$\langle 0.5, 0.3, 0.1 \rangle$	$\langle 0.4, 0.1, 0.5 \rangle$	$\langle 0.5, 0.3, 0.1 \rangle$	$\langle 0.5, 0.3, 0.1 \rangle$...	$\langle 0.5, 0.3, 0.1 \rangle$	$\langle 0.5, 0.3, 0.1 \rangle$	$\langle 0.5, 0.3, 0.1 \rangle$	$\langle 0.5, 0.3, 0.1 \rangle$

Then the weighted hamming distance measure (WHDM) [37] between NS_{Feat}^{Im} and α^{IP} is defined by:

$$d(NS_{Feat_i}^{Im}, \alpha^{IP}) = \sum_{k=1}^S \lambda_k \sum_{j=1}^n d(NS_{ij}^{Im^k}, \alpha_j^{IP})$$

The proposed programming model is established:

$$\min f(w) = \sum_{k=1}^S \lambda_k \sum_{i=1}^m \sum_{j=1}^n w_j d(NS_{Feat_{ij}}^{Im}, NS_{Feat.}^Q) \dots (3)$$

With constraints:

$$\begin{aligned} \sum_{j=1}^n w_j^2 &= 1, \\ w_j &\geq 0 \text{ where } j = 1, 2, \dots, n \end{aligned}$$

To solve the model, the Lagrange function [38] as the follows:

$$\mathcal{L}(w, \mathfrak{L}) = \sum_{k=1}^S \lambda_k \sum_{i=1}^m \sum_{j=1}^n w_j d(NS_{Feat_{ij}}^{Im}, NS_{Feat.}^Q) + \frac{\mathfrak{L}}{2} \left(\sum_{j=1}^n w_j^2 - 1 \right) \dots (4)$$

Where; \mathfrak{L} is the Lagrange multiplier.

The following equations can obtained through differentiating with respect to w_j and \mathfrak{L} of the previous equation and setting the partial differentiation equal to zero as:

$$\begin{aligned} \frac{\partial \mathcal{L}}{\partial w_j} &= \sum_{k=1}^S \lambda_k \sum_{i=1}^m d(NS_{Feat_{ij}}^{Im}, \alpha_j^{IP}) + w_j \mathcal{L} = 0 \\ \frac{\partial \mathcal{L}}{\partial \lambda} &= \sum_{j=1}^n w_j^2 = 1 \end{aligned}$$

The value of the weight (w_j) can be obtained from the solution of the two previous equations, then normalize it as:

$$w_j^* = \frac{w_j}{\sum_{j=1}^n w_j}$$

Then;

$$w_j^* = \frac{\sum_{k=1}^S \lambda_k \sum_{i=1}^m d(NS_{Feat_{ij}}^{Im}, NS_{Feat.}^Q)}{\sum_{j=1}^n \sum_{k=1}^S \lambda_k \sum_{i=1}^m d(NS_{Feat_{ij}}^{Im}, NS_{Feat.}^Q)} \dots (5)$$

The optimal solution $w^* = (w_1^*, w_2^*, \dots, w_n^*)$ is getting which is considered as the weight of the features. Then, the closest image to the query is the calculated minimum distance from the equation 1.

Illustrative Example: Suppose that the features of four images where each image have four objects, each object have four features, were extracted using the proposed system as follows:

$$\begin{aligned} Im_1 &= \begin{bmatrix} \langle 0.4, 0.3, 0.3 \rangle & \langle 0.4, 0.2, 0.3 \rangle & \langle 0.2, 0.2, 0.5 \rangle & \langle 0.7, 0.2, 0.3 \rangle \\ \langle 0.6, 0.1, 0.2 \rangle & \langle 0.6, 0.1, 0.2 \rangle & \langle 0.5, 0.2, 0.3 \rangle & \langle 0.5, 0.1, 0.2 \rangle \\ \langle 0.3, 0.2, 0.3 \rangle & \langle 0.5, 0.2, 0.3 \rangle & \langle 0.1, 0.5, 0.2 \rangle & \langle 0.1, 0.4, 0.5 \rangle \\ \langle 0.7, 0.2, 0.1 \rangle & \langle 0.6, 0.1, 0.2 \rangle & \langle 0.4, 0.3, 0.2 \rangle & \langle 0.4, 0.5, 0.1 \rangle \end{bmatrix} \\ Im_2 &= \begin{bmatrix} \langle 0.1, 0.3, 0.5 \rangle & \langle 0.5, 0.1, 0.5 \rangle & \langle 0.3, 0.1, 0.6 \rangle & \langle 0.4, 0.1, 0.4 \rangle \\ \langle 0.2, 0.5, 0.4 \rangle & \langle 0.3, 0.4, 0.3 \rangle & \langle 0.2, 0.3, 0.1 \rangle & \langle 0.2, 0.3, 0.5 \rangle \\ \langle 0.5, 0.2, 0.6 \rangle & \langle 0.2, 0.4, 0.3 \rangle & \langle 0.5, 0.2, 0.5 \rangle & \langle 0.1, 0.5, 0.3 \rangle \\ \langle 0.2, 0.4, 0.2 \rangle & \langle 0.1, 0.1, 0.3 \rangle & \langle 0.1, 0.5, 0.4 \rangle & \langle 0.5, 0.3, 0.1 \rangle \end{bmatrix} \\ Im_3 &= \begin{bmatrix} \langle 0.3, 0.2, 0.1 \rangle & \langle 0.3, 0.1, 0.3 \rangle & \langle 0.1, 0.4, 0.5 \rangle & \langle 0.2, 0.3, 0.5 \rangle \\ \langle 0.6, 0.1, 0.4 \rangle & \langle 0.6, 0.4, 0.2 \rangle & \langle 0.5, 0.4, 0.1 \rangle & \langle 0.5, 0.2, 0.4 \rangle \\ \langle 0.3, 0.3, 0.6 \rangle & \langle 0.4, 0.2, 0.4 \rangle & \langle 0.2, 0.3, 0.2 \rangle & \langle 0.3, 0.5, 0.1 \rangle \\ \langle 0.3, 0.6, 0.1 \rangle & \langle 0.5, 0.3, 0.2 \rangle & \langle 0.3, 0.3, 0.6 \rangle & \langle 0.4, 0.3, 0.2 \rangle \end{bmatrix} \\ Im_4 &= \begin{bmatrix} \langle 0.2, 0.2, 0.3 \rangle & \langle 0.3, 0.2, 0.3 \rangle & \langle 0.2, 0.3, 0.5 \rangle & \langle 0.4, 0.2, 0.5 \rangle \\ \langle 0.4, 0.1, 0.2 \rangle & \langle 0.6, 0.3, 0.5 \rangle & \langle 0.1, 0.2, 0.2 \rangle & \langle 0.5, 0.1, 0.2 \rangle \\ \langle 0.3, 0.5, 0.1 \rangle & \langle 0.2, 0.2, 0.3 \rangle & \langle 0.5, 0.4, 0.3 \rangle & \langle 0.5, 0.3, 0.2 \rangle \\ \langle 0.3, 0.1, 0.1 \rangle & \langle 0.2, 0.1, 0.4 \rangle & \langle 0.2, 0.3, 0.2 \rangle & \langle 0.3, 0.1, 0.6 \rangle \end{bmatrix} \end{aligned}$$

Suppose that $\alpha_j^{IP} = \{1, 0, 0\}$ be four ideal SVNNS, then a SVNPIs is defined by:

$$\alpha^{IP} = [\alpha_1^{IP}, \alpha_2^{IP}, \alpha_3^{IP}, \alpha_4^{IP}]$$

Step 1: By applying the proposed model:

$$\min f(w) = 1.5833w_1 + 1.5038w_2 + 1.825w_3 + 1.625w_4$$

And constraints are:

$$\begin{aligned} \sum_{j=1}^4 w_j^2 &= 1 \\ w_j &\geq 0, \quad j = 1, 2, 3, 4 \end{aligned}$$

Step 2: Calculate the weight vector attribute by using equation 5:

$$w_1 = 0.18, w_2 = 0.22, w_3 = 0.30, w_4 = 0.30$$

Step 3: Suppose that the feature of the query image is:

$$Im_Q = \begin{bmatrix} \langle 0.5, 0.3, 0.5 \rangle & \langle 0.5, 0.1, 0.5 \rangle & \langle 0.3, 0.1, 0.6 \rangle & \langle 0.4, 0.1, 0.4 \rangle \\ \langle 0.2, 0.5, 0.4 \rangle & \langle 0.3, 0.2, 0.3 \rangle & \langle 0.2, 0.3, 0.1 \rangle & \langle 0.2, 0.4, 0.5 \rangle \\ \langle 0.5, 0.2, 0.6 \rangle & \langle 0.2, 0.4, 0.3 \rangle & \langle 0.5, 0.2, 0.5 \rangle & \langle 0.1, 0.5, 0.3 \rangle \\ \langle 0.2, 0.4, 0.1 \rangle & \langle 0.1, 0.1, 0.3 \rangle & \langle 0.1, 0.3, 0.4 \rangle & \langle 0.5, 0.3, 0.1 \rangle \end{bmatrix}$$

By using equations 1 and 2, the distance measures are:

$$d(NS_{Feat_{ij}}^{Im}, NS_{Feat.}^Q)^1 = 0.4352$$

$$d(NS_{Feat_{ij}}^{Im}, NS_{Feat.}^Q)^2 = 0.3613$$

$$d(NS_{Feat_{ij}}^{Im}, NS_{Feat.}^Q)^3 = 0.4482$$

$$d(NS_{Feat_{ij}}^{Im}, NS_{Feat.}^Q)^4 = 0.3984$$

Step 4: The ascending ordered are used to rank the results as:

$$NS_2^{Im} > NS_4^{Im} > NS_1^{Im} > NS_3^{Im}$$

The closest image from alternative images to query image is image number two.

7. Experimental work:

The Wang image database [39] is used to evaluate the proposed system. Wang image database consists of 10,000 generic images with 256x384 pixels or 384x256 pixels size. The proposed system consists ten categories that derived from the main images database. The categories are Butterfly, Cars, Dinosaurs, Texture, Sunset, Flowers, Mountain, Horses, Forests, and Elephant as shown in figure 8.



Fig. 8: WBIIS images database.

Both the images, whether in the database or a query passed through the steps that will be displayed later on one of the images in the database as shown in the table 2.

Features of images ($NS_{Feat.}^{Im}$) are stored in categories that are clustered with corresponding identifier indicating to the number of objects in the image ($NS_{Feat.}^{Obj_n}$).

8. Results and discussion:

8.1. Performance evaluation:






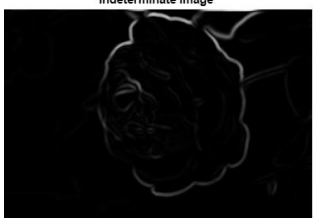


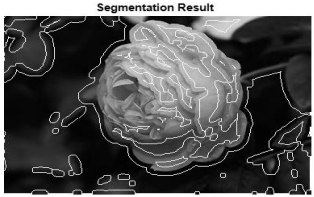
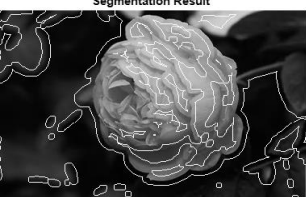

The proposed system is evaluated focusing on the accuracy and robustness to uncertainty image segmentation.

A. Accuracy:

The important accuracy measures used in evaluation the systems performance are precision, recall and f-measure [40].

$$\begin{aligned} \text{Precision } (P) &= \frac{\text{No. of relevant images retrieved}}{\text{Total No. of images retrieved}} \\ \text{Recall } (R) &= \frac{\text{No. of relevant images retrieved}}{\text{Total No. of relevant images}} \\ F_{\text{measure}} &= \frac{2 \times R \times P}{R + P} \end{aligned}$$

Table 2: the procedures that achieved from original image to feature extracted

Processing		Input image	Procedures	Output image
Image pre-processing			A color image is converted to a gray image.	
Neutrosophic Image Domain	T-Domain		Determine membership and non-membership degree (T and F).	
	F-Domain			
	I-Domain		Determine indeterminacy (I) according to homogeneity as in section 2.	
Neurtosophic binary image		Both binarized T-domain, F-domain and indeterminacy domain are used.	According to Th_T, Th_F and Th_I .	
Optimal segmentation boundaries			By using the watershed algorithm.	
Neutrosophic image segmented			By using neutrosophic image processing.	
Features Extraction		From segmented image feature is extracting for each objects as in section 3.		

But in the recently, the common measures are the average precision which provides across the recall levels a single figure measure of quality.

Where research proved, especially in the field of texts that this measure is characterized by good discrimination and stability [41]. For single query image, the average precision is the mean cross he precision scores after each retrieved relevant images:

$$\text{Average precision } (P_{Av.}) = \frac{1}{N_R} \sum_{n=1}^{N_n} P_q(R_n)$$

Where, R_n is the recall after the n^{th} relevant image was retrieved, N_R is the total number of the query relevant image. Over all queries the mean average precision means the average precision scores:

$$P_{MAv.} = \frac{1}{|Q|} \sum_{q \in Q} P_{Av.}(q) \dots (6)$$

Where Q is a set of queries.

Additionally, they are two statistics measures are computed for the query image namely mean rank (R_{mean}^i) and the standard deviation (σ^i) of all the matched images [42].

$$R_{mean}^i = \frac{1}{N_R} \sum_{n=1}^{N_n} r(i, j) \dots (7)$$

Where $r(i, j)$ the image (j) position in the retrieved images for query (i).

$$\sigma^i = \left[\frac{1}{N_R} \sum_{n=1}^{N_n} (r(i, j) - R_{mean}^i)^2 \right]^{0.5} \dots (8)$$

Similarly, the average mean rank and the average standard deviation for all images in database are defined as:

$$AR_{mean} = \frac{1}{|Q|} \sum_{q \in Q} r(q) \dots (9)$$

$$A\sigma = \frac{1}{|Q|} \sum_{q \in Q} \sigma(q) \dots (10)$$

B. Uncertainty Segmentation Robustness:

Uncertainty regions that constructed from an intersection between objects in the image are used the entropy measures to characterize where the larger value of entropy, the higher the uncertainty level. For each image (Im_i) has (S_r) segmented regions, its entropy ($Ent(Im_i)$) is:

$$Ent(Im_i) = - \sum_{j=1}^{S_r} P(\mathfrak{R}_j^{Im_i}) \log [P(\mathfrak{R}_j^{Im_i})] \dots (11)$$

Where; $P(\mathfrak{R}_j^{Im_i})$ is the image percentage covered by region $\mathfrak{R}_j^{Im_i}$.

Accordingly, the overall average entropy for all images in the database is defined as:

$$AEnt = \frac{1}{N_R} \sum_{i=1}^{N_n} Ent(Im_i)$$

8.2. Experimental results:

The similarities in the proposed system are based on the similarity between the constituent objects of the image. One of the disadvantages of this method is that an object in one image can correspond to several objects in another image. This is due to several reasons, one of them that image segmentation is not ideal. So neutrosophy theory has been used with WHDM to solve the similarity problem. Where neutrosophic image processing is used because it has the advantage of identifying uncertainly objects as shown in sections 3 and 4. The proposed system used the Matlab Version: 9.0.0.341360 (R2016a) program to build the database through the processing of the neutrosophic images as shown in figure 9 and extracting the image attributes and saving them in the database.

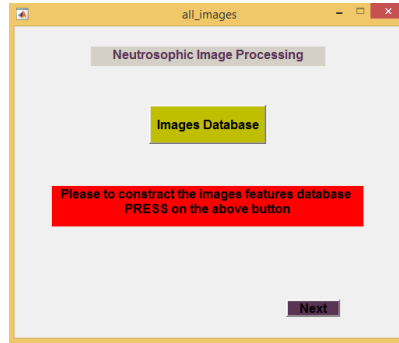


Fig. 9: Features of image database preparation.

The query image is treated in the same way, then the query image is classified according to its objects number and computed their neutrosophic features. The weight distance measure is used to match the query image features with categorized features image database. The excel solver was used to determine the ideal weight values used in the matching process and the results were as shown in Figures 10-a, 10-b, and 10-c.

Cell	Name	Original Value	Final Value
\$C\$15	z w1	1.306786442	1.306786442

Cell	Name	Original Value	Final Value	Integer
\$C\$14	solution w1	0.143075485	0.143075485	Contin
\$D\$14	solution w2	0.280827768	0.280827768	Contin
\$E\$14	solution w3	0.667295857	0.667295857	Contin
\$F\$14	solution w4	0.674819879	0.674819879	Contin

Cell	Name	Cell Value	Formula	Status	Slack
\$H\$10		0.881843375	\$H\$10 >= \$J\$10	Not Binding	0.881843375
\$H\$11		1.000000459	\$H\$11 = \$J\$11	Binding	0
\$H\$7		0.186956879	\$H\$7 = \$J\$7	Not Binding	0.186956879
\$H\$8		0.366995348	\$H\$8 = \$J\$8	Not Binding	0.366995348
\$H\$9		0.872011367	\$H\$9 = \$J\$9	Not Binding	0.872011367

Fig.10-a: Answer report for excel solver result.

Cell	Name	Final Value	Reduced Gradient
\$C\$14	solution w1	0.143075485	0
\$D\$14	solution w2	0.280827768	0
\$E\$14	solution w3	0.667295857	0
\$F\$14	solution w4	0.674819879	0

Cell	Name	Final Value	Lagrange Multiplier
\$H\$10		0.881843375	0
\$H\$11		1.000000459	0.65339104
\$H\$7		0.186956879	0
\$H\$8		0.366995348	0
\$H\$9		0.872011367	0

Fig.10-b: Sensitivity report for excel solver result.

Microsoft Excel 15.0 Limits Report
Worksheet: [weight calculation.xlsx]Sheet6
Report Created: 02/01/2019 08:12:14

Objective	
Cell	Name Value
\$C\$15	z w1 1.306786442

Cell	Variable Name	Value	Lower Limit	Objective Result	Upper Limit	Objective Result
\$C\$14:\$F\$14						
\$C\$14	solution w1	0.143075485	0.143075485	1.306786442	0.143075485	1.306786442
\$D\$14	solution w2	0.280827768	0.280827768	1.306786442	0.280827768	1.306786442
\$E\$14	solution w3	0.667295857	0.667295857	1.306786442	0.667295857	1.306786442
\$F\$14	solution w4	0.674819879	0.674819879	1.306786442	0.674819879	1.306786442

Fig.10-c: Limits report for excel solver result.

The proposed system was evaluated using the common standard measures of precision, recall, and f-measure, where only 5 matches were shown for each query image as shown in figure 11. The attached program can be used to obtain more matching using the attached query images to repeat the retrieval.

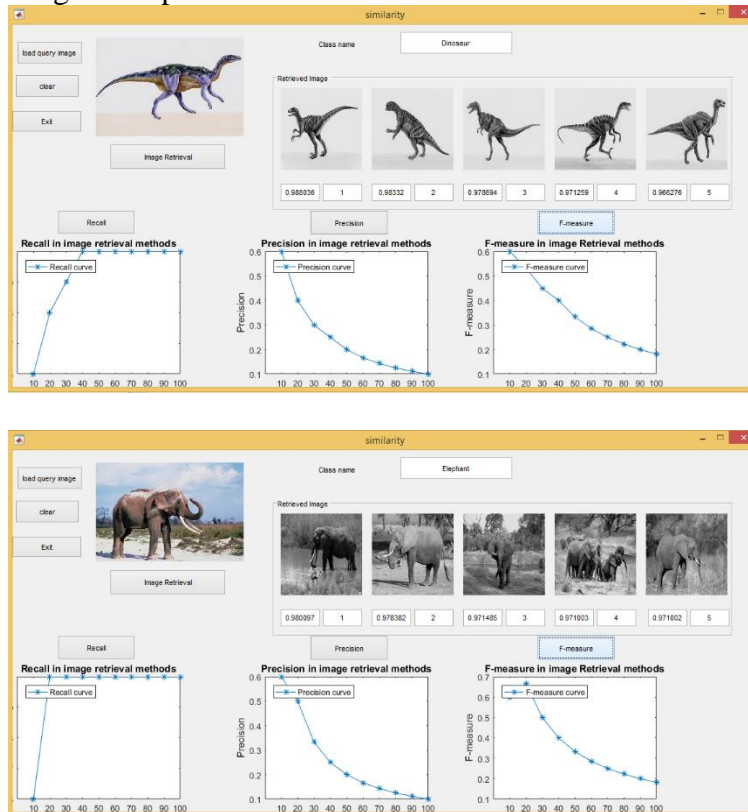


Fig.11: The proposed system evaluation examples.

To evaluate image quality based on the number of objects in the image, the lower rank, the better performance. For this to be done, both the average precision and the mean rank must be the maximum and the minimum, respectively. Figure 12 shows the average of precision, rank, and standard deviation.

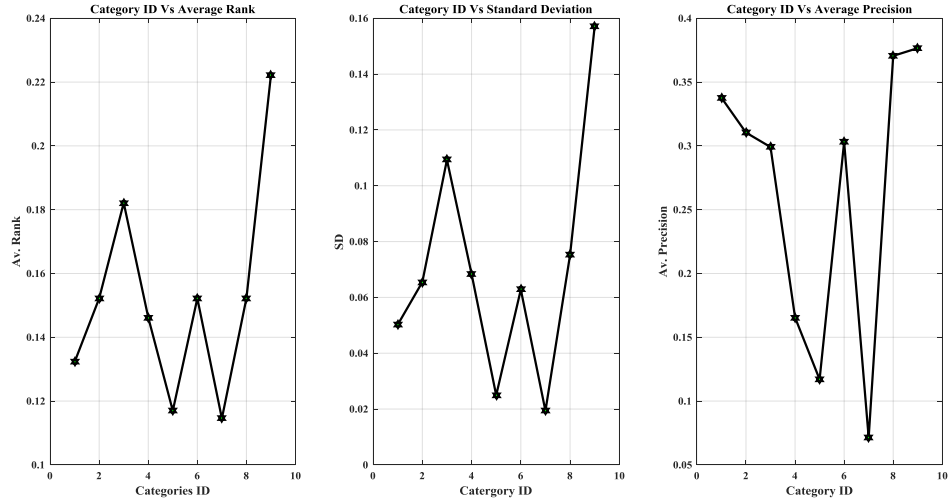


Fig. 12: category ID with respect to average rank, standard deviation, and average precision.

The best performance was achieved at the precision = 1 and the mean rank = 0.1. This was done with the single-object image such dinosaur (mean rank=0.11 with standard deviation = 0.07) and elephant (mean rank=0.12 with standard deviation = 0.02) as shown in Fig. 12. Although precision = 1, the mean rank was high (mean rank =0.2 11 with standard deviation = 0.15), resulting in a mismatch with the result as shown in Figure 13.

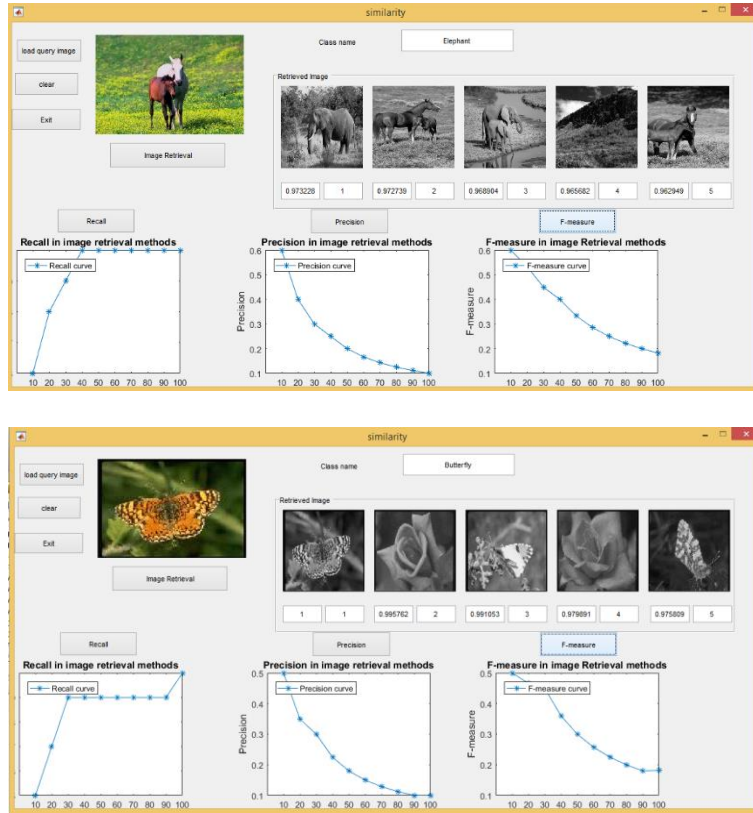


Fig. 13: matching disagree for the multi-objects image example.

The naturopathic features of images are characterized by their ability to identify similarities between overlapping and uncertainty objects. As shown in figure 14, the

proposed method with multi-objects is achieved a good performance where precision =1 and the mean rank = 0.12 with standard deviation =0.017.

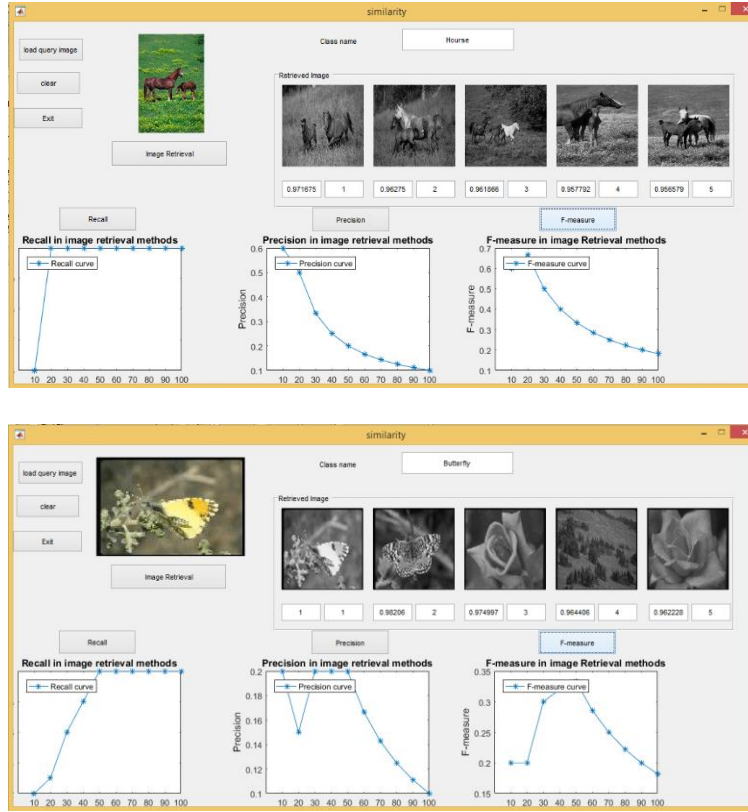


Fig. 14: The multi-objects matching by the proposed system.

Figure 14 shows the improvement in image retrieval due to the use of the proposed system, which is characterized by accurate image segmentation, which increases the entropy as shown by Figure 15.

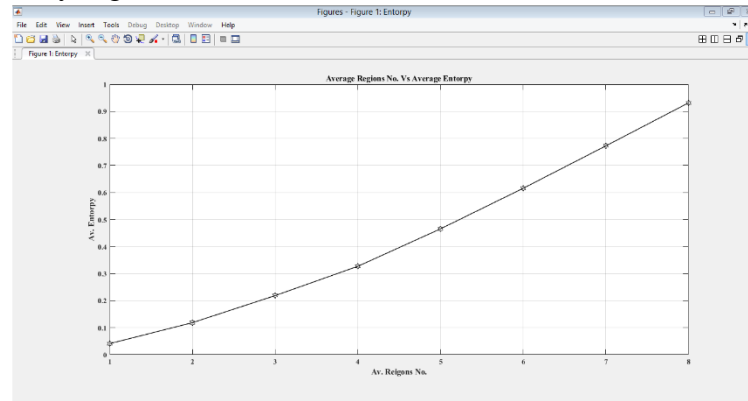


Fig. 15: overall average entropy.

The lower the entropy the lower the levels of uncertainty, which leads to increase the precision in retrieving images while preserving the details in the original image.

From the above, the proposed system performs is effective in retrieving images with high accuracy. By comparing the proposed system with the other similar methods based on distance measures such as Euclidian, Manhattan, and Minkowski, provided the better result as shown in Table 3.

Table 3: comparison between distances measuring with proposed.

Methods Type of Database	Euclidean		Manhattan		Minkowski		Proposed Method	
	P%	R%	P%	R%	P%	R%	P%	R%
Butterfly	0.1629	0.7400	0.1626	0.7900	0.1461	0.7200	0.1901	0.8300
Car	0.1801	0.8100	0.1746	0.8000	0.1347	0.7300	0.1842	0.8200
Dinosaur	0.2829	0.9900	0.1059	0.6000	0.2829	0.9900	0.2829	0.9900
Elephant	0.2329	0.9300	0.2229	0.9200	0.2329	0.9400	0.2179	0.9500
Flowers	0.1871	0.7900	0.1684	0.7800	0.1742	0.8200	0.1646	0.8300
Forests	0.1579	0.7400	0.1552	0.7400	0.1461	0.7000	0.2028	0.8300
Horses	0.2779	0.9800	0.2779	0.9800	0.2679	0.9700	0.0915	0.9800
Mountain	0.1574	0.7400	0.1439	0.7200	0.2079	0.9100	0.1497	0.7500
Sunset	0.1142	0.6300	0.2251	0.8800	0.1392	0.7400	0.1937	0.8500
Texture	0.2446	0.8900	0.2296	0.8700	0.2496	0.8900	0.2070	0.7900

The results showed the high performance in the images retrieval with high accuracy, which exceeded all other measures, where the results were excellent in cases of single-object images, such as dinosaurs and some elephants, where the recall was 99% and 95% respectively. While in multi-object images, the rate of retrieval of images was very good as is evident in the images of forests, sunset, and horses where the results respectively are 83%, 85%, 98%.

9. Conclusion

A novel similarity model used to match the neutrosophic image features for CBIRs. In the proposed system, an image is segmented into objects, edges and background by using neutrosophic image processing. Each object is then represented by a neutrosophic features that is determined by set of degree of truth, indeterminacy, and falsity. Where, the membership functions of truth, indeterminacy and falsity naturally characterizes the gradual transition between objects within image. That meaning, it distinguishes the uncertainly regions because of the overlap of objects with each other or because of inaccurate segmentation. To retrieval the query image from the images database, weighted humming distance measure is used. Single-valued neutrosophic ideal solution is defined then the optimal features weight is established. The comparison results between the proposed model and others distance measures show that the proposed similarity model is reasonable and effective in dealing with image retrieval.

References

- [1] Li, Xirong, et al. "Socializing the semantic gap: A comparative survey on image tag assignment, refinement, and retrieval." *ACM Computing Surveys (CSUR)* 49.1 (2016): 14.
- [2] Luo, Jake, et al. "Big data application in biomedical research and health care: a literature review." *Biomedical informatics insights* 8 (2016): BII-S31559.
- [3] Bala, Anu, and Tajinder Kaur. "Local texton XOR patterns: A new feature descriptor for content-based image retrieval." *Engineering Science and Technology, an International Journal* 19.1 (2016): 101-112.
- [4] Baeza-Yates, Ricardo, and Berthier de Araújo Neto Ribeiro. *Modern information retrieval*. New York: ACM Press; Harlow, England: Addison-Wesley, 2011.
- [5] Lin, Yuanqing, et al. "Large-scale image classification: fast feature extraction and svm training." *Computer Vision and Pattern Recognition (CVPR), 2011 IEEE Conference on*. IEEE, 2011.

- [6] ping Tian, Dong. "A review on image feature extraction and representation techniques." *International Journal of Multimedia and Ubiquitous Engineering* 8.4 (2013): 385-396.
- [7] Collins, John, and Kazunori Okada. "A Comparative Study of Similarity Measures for Content-Based Medical Image Retrieval." *CLEF (Online Working Notes/Labs/Workshop)*. 2012.
- [8] Ramsey, Fred, and Daniel Schafer. *The statistical sleuth: a course in methods of data analysis*. Cengage Learning, 2012.
- [9] Hau, Chen Chi, ed. *Handbook of pattern recognition and computer vision*. World Scientific, 2015.
- [10] Wang, Xiaoyue, et al. "Experimental comparison of representation methods and distance measures for time series data." *Data Mining and Knowledge Discovery* 26.2 (2013): 275-309.
- [11] Bausys, Romualdas, and Edmundas-Kazimieras Zavadskas. *Multicriteria decision making approach by VIKOR under interval neutrosophic set environment*. Infinite Study, 2015.
- [12] Smarandache, Florentin. *n-Valued Refined Neutrosophic Logic and Its Applications to Physics*. Infinite Study, 2013.
- [13] Smarandache, Florentin. *Neutrosophic Perspectives: Triplets, Duplets, Multisets, Hybrid Operators, Modal Logic, Hedge Algebras. And Applications*. Infinite Study, 2017.
- [14] Ye, Jun. "Single valued neutrosophic cross-entropy for multicriteria decision making problems." *Applied Mathematical Modelling* 38.3 (2014): 1170-1175.
- [15] Smarandache, Florentin. *(t, i, f)-Neutrosophic Structures & I-Neutrosophic Structures (Revisited)*. Infinite Study, 2015.
- [16] Ye, Jun. "Similarity measures between interval neutrosophic sets and their applications in multicriteria decision-making." *Journal of Intelligent & Fuzzy Systems* 26.1 (2014): 165-172.
- [17] Cheng, H. D., Yanhui Guo, and Yingtao Zhang. "A novel image segmentation approach based on neutrosophic set and improved fuzzy c-means algorithm." *New Mathematics and Natural Computation* 7.01 (2011): 155-171.
- [18] Hasikin, Khairunnisa, and Nor Ashidi Mat Isa. "Enhancement of the low contrast image using fuzzy set theory." *Computer Modelling and Simulation (UKSim), 2012 UKSim 14th International Conference on*. IEEE, 2012.
- [19] Liang, Kun, et al. "A new adaptive contrast enhancement algorithm for infrared images based on double plateaus histogram equalization." *Infrared Physics & Technology* 55.4 (2012): 309-315.
- [20] Wulfmeier, Markus, Peter Ondruska, and Ingmar Posner. "Maximum entropy deep inverse reinforcement learning." arXiv preprint arXiv: 1507.04888 (2015).
- [21] Caplin, Andrew, Mark Dean, and John Leahy. Rationally inattentive behavior: Characterizing and generalizing Shannon entropy. No. w23652. National Bureau of Economic Research, 2017.
- [22] Shan, Juan, H. D. Cheng, and Yuxuan Wang. "A novel segmentation method for breast ultrasound images based on neutrosophic l-means clustering." *Medical physics* 39.9 (2012): 5669-5682.

- [23] Nercessian, Shahan C., Karen A. Panetta, and Sos S. Agaian. "Non-linear direct multi-scale image enhancement based on the luminance and contrast masking characteristics of the human visual system." *IEEE Transactions on image processing* 22.9 (2013): 3549-3561.
- [24] Nikolova, Mila, and Gabriele Steidl. "Fast hue and range preserving histogram specification: Theory and new algorithms for color image enhancement." *IEEE transactions on image processing* 23.9 (2014): 4087-4100.
- [25] Panetta, Karen, et al. "Parameterized logarithmic framework for image enhancement." *IEEE Transactions on Systems, Man, and Cybernetics, Part B (Cybernetics)* 41.2 (2011): 460-473.
- [26] Jung, Seung-Won, Le Thanh Ha, and Sung-Jea Ko. "A new histogram modification based reversible data hiding algorithm considering the human visual system." *IEEE Signal Process. Lett.* 18.2 (2011): 95-98.
- [27] Guo, Yanhui, et al. "A novel image segmentation approach based on neutrosophic c-means clustering and indeterminacy filtering." *Neural Computing and Applications* 28.10 (2017): 3009-3019.
- [28] Vairalkar, Manoj K., and S. U. Nimbhorkar. "Edge detection of images using sobel operator." *International Journal of Emerging Technology and Advanced Engineering* 2.1 (2012): 291-293.
- [29] Sengur, Abdulkadir, and Yanhui Guo. "Color texture image segmentation based on neutrosophic set and wavelet transformation." *Computer Vision and Image Understanding* 115.8 (2011): 1134-1144.
- [30] Guo, Yanhui, Abdulkadir Şengür, and Jun Ye. "A novel image thresholding algorithm based on neutrosophic similarity score." *Measurement* 58 (2014): 175-186.
- [31] Arbelaez, Pablo, et al. "Contour detection and hierarchical image segmentation." *IEEE transactions on pattern analysis and machine intelligence* 33.5 (2011): 898-916.
- [32] Couprie, Camille, et al. "Power watershed: A unifying graph-based optimization framework." *IEEE transactions on pattern analysis and machine intelligence* 33.7 (2011): 1384-1399.
- [33] de Siqueira, Fernando Roberti, William Robson Schwartz, and Helio Pedrini. "Multi-scale gray level co-occurrence matrices for texture description." *Neurocomputing* 120 (2013): 336-345.
- [34] Alçin, Ömer F., et al. "Multi-category EEG signal classification developing time-frequency texture features based Fisher Vector encoding method." *Neurocomputing* 218 (2016): 251-258.
- [35] Broumi, Said, and Florentin Smarandache. *Several similarity measures of neutrosophic sets*. Infinite Study, 2013.
- [36] Broumi, Said, and Florentin Smarandache. *New distance and similarity measures of interval neutrosophic sets*. Infinite Study, 2014.
- [37] Liao, Huchang, and Zeshui Xu. "Approaches to manage hesitant fuzzy linguistic information based on the cosine distance and similarity measures for HFLTSSs and their application in qualitative decision making." *Expert Systems with Applications* 42.12 (2015): 5328-5336.

- [38] Faddeev, Ludvig D., and Victor N. Popov. "Feynman diagrams for the Yang-Mills field." *Fifty Years of Mathematical Physics: Selected Works of Ludwig Faddeev*. 2016. 157-158.
- [39] Jia Li and James Z. Wang, ``Real-time Computerized Annotation of Pictures," *IEEE Transactions on Pattern Analysis and Machine Intelligence*, vol. 30, no. 6, pp. 985-1002, 2008.
- [40] Powers, David Martin. "Evaluation: from precision, recall and F-measure to ROC, informedness, markedness and correlation." (2011).
- [41] Zhai, Chengxiang, and John Lafferty. "A study of smoothing methods for language models applied to ad hoc information retrieval." *ACM SIGIR Forum*. Vol. 51. No. 2. ACM, 2017.
- [42] Weston, Jason, Samy Bengio, and Nicolas Usunier. "Wsabie: Scaling up to large vocabulary image annotation." *IJCAI*. Vol. 11. 2011.